




Tubular TMEM16A promotes tubulointerstitial fibrosis by suppressing PGC-1 α -mediated mitochondrial homeostasis in diabetic kidney disease

Jia-Ling Ji¹ · Jun-Ying Li² · Jian-Xiang Liang³ · Yan Zhou⁴ · Cong-Cong Liu² · Yao Zhang² · Ai-Qing Zhang¹ · Hong Liu⁴ · Rui-Xia Ma² · Zuo-Lin Li⁴ 

Received: 14 July 2023 / Revised: 18 September 2023 / Accepted: 10 October 2023 / Published online: 6 November 2023

© The Author(s), under exclusive licence to Springer Nature Switzerland AG 2023

Abstract

Tubulointerstitial fibrosis (TIF) plays a crucial role in the progression of diabetic kidney disease (DKD). However, the underlying molecular mechanisms remain obscure. The present study aimed to examine whether transmembrane member 16A (TMEM16A), a Ca²⁺-activated chloride channel, contributes to the development of TIF in DKD. Interestingly, we found that TMEM16A expression was significantly up-regulated in tubule of murine model of DKD, which was associated with development of TIF. In vivo inhibition of TMEM16A channel activity with specific inhibitors Ani9 effectively protects against TIF. Then, we found that TMEM16A activation induces tubular mitochondrial dysfunction in in vivo and in vitro models, with the evidence of the TMEM16A inhibition with specific inhibitor. Mechanically, TMEM16A mediated tubular mitochondrial dysfunction through inhibiting PGC-1 α , whereas overexpression of PGC-1 α could rescue the changes. In addition, TMEM16A-induced fibrogenesis was dependent on increased intracellular Cl⁻, and reducing intracellular Cl⁻ significantly blunted high glucose-induced PGC-1 α and profibrotic factors expression. Taken together, our studies demonstrated that tubular TMEM16A promotes TIF by suppressing PGC-1 α -mediated mitochondrial homeostasis in DKD. Blockade of TMEM16A may serve as a novel therapeutic approach to ameliorate TIF.

Keywords TMEM16A · Tubulointerstitial fibrosis · PGC-1 α · Mitochondrial dysfunction · Intracellular Cl⁻

Jia-Ling Ji and Jun-Ying Li contributed equally to this work.

✉ Hong Liu
jstzliu@sina.com

✉ Rui-Xia Ma
anita1685@163.com

✉ Zuo-Lin Li
zuolin_li1990@126.com

¹ Department of Pediatrics, The Fourth Affiliated Hospital of Nanjing Medical University, Nanjing, Jiangsu, China

² Department of Nephrology, The Affiliated Hospital of Qingdao University, Qingdao, Shandong, China

³ Department of Ultrasonography, Weifang People's Hospital, Weifang, Shandong, China

⁴ Institute of Nephrology, Zhongda Hospital, Southeast University School of Medicine, Nanjing, Jiangsu, China

Introduction

Diabetic kidney disease (DKD), as one of the fastest growing causes of chronic kidney disease, is the major cause of end-stage renal disease worldwide and is associated with a high morbidity and mortality. Accumulating evidence indicates that the pathogenesis of DKD involves multifactorial processes (including hyperglycemia-induced metabolic alterations, mitochondrial dysfunction, and inflammation) that converge to initiate and advance the disease. Although the clinical therapy of DKD has made great progress [1, 2]; unfortunately, the progression of DKD still cannot effectively inhibited. Therefore, further exploring the pathogenesis of DKD and improving the therapeutic outcomes are unmet.

Tubulointerstitial fibrosis (TIF), one of the most common characteristic pathological features, plays a crucial role in the progression of DKD [3]. TIF is characterized by the deposition of extracellular matrix (ECM), including fibronectin (FN) and collagen-1. Growing evidence demonstrates

that in response to injury, tubular epithelial cells undergo changes and function as fibrogenic cells with the consequent production of various bioactive molecules, leading to ECM remodelling and development of TIF in DKD [4, 5]. However, the molecular mechanisms underlying tubule-mediated TIF in DKD remain incompletely understood. Elucidating the exact mechanisms of tubule-mediated TIF in DKD has very important significance in providing new therapeutic strategies to retard the progression of DKD.

The calcium-activated chloride channel, transmembrane member 16A (TMEM16A), is ubiquitously expressed in almost all tissues and is essential to maintaining physiological functions, such as epithelial secretion, smooth muscle contraction and sensory signal transduction [6, 7]. Emerging pieces of evidence found that TMEM16A contributes to the regulation of renal proximal tubular proton secretion and protein reabsorption [8]. Recently, TMEM16A may also function as a potential therapeutic target for delay of cyst development in polycystic kidney disease [9], suggesting an important function of TMEM16A in renal pathophysiology. However, whether TMEM16A is involved in TIF in DKD is still unknown.

Thereby, in this study, we aim to explore the functional effects of TMEM16A on TIF in DKD. Interestingly, we found that tubular TMEM16A expression was significantly increased, promoting the development of TIF in DKD. Mechanistically, we demonstrated that activation of TMEM16A induced mitochondrial dysfunctions through inhibiting peroxisome proliferator-activated receptor- γ co-activator-1 α (PGC-1 α) during TIF. Collectively, a previously unrecognized mechanism of TIF development in DKD was elucidated. Our findings provide a novel therapeutic target for preventing DKD.

Methods and materials

Animals

The experimental procedures were approved by the ethics review committee for animal experiment of Southeast University. Experiments were conducted using 8-week-old male C57BLKS/JLepr background db/db mice (43–45 g) as the DKD model and their age-matched heterozygous male db/m mice as a control, which were all purchased from GemPharmatech LLC (Nanjing, China). Renal pathology was evaluated at 20 weeks of age, and renal function worsened, accompanied by glomerular enlargement, diffuse expansion of mesangial matrix and TIF. These mice were randomly divided into several groups according to the experimental protocol and were allowed free access to the same diet under the same conditions.

In vivo TMEM16A inhibitor Ani9 treatments and lentiviral transduction

To inhibit TMEM16A, beginning at 12 weeks of age, db/db mice were subjected to daily intraperitoneal injections of Ani9 (a specific TMEM16A inhibitor [9], Selleck Chemicals LLC, Houston, TX, USA) or vehicle (PBS) at 5 mg/kg body weight for 8 consecutive weeks. For lentiviral gene transfer, lentiviruses overexpression targeting PGC-1 α (Lv-PGC-1 α) and negative control (Lv-NC) were purchased from GenePharma (Shanghai, China). Beginning at 12 weeks of age, Lv-mediated gene transfer in the kidneys of db/db mice was performed by the tail vein injection once a week for 8 weeks (5×10^9 TU/mouse). All mice were sacrificed at 20 weeks of age and their serum and kidneys were harvested.

Kidney histology

For histology analysis, kidneys were fixed with 4% formalin, embedded in paraffin, and sectioned to 4- μ m thickness. Renal sections were used for Masson's trichrome staining. To evaluate TIF, at least five random tissue sections per mouse were assessed on Masson's trichrome staining. Tissue fibrosis as defined by blue staining was scored by three experienced observers masked to experiment conditions, and the average values of the fibrosis scores were reported.

Immunohistochemistry staining

For immunohistochemistry, kidney sections were incubated with primary antibodies against anti-TMEM16A (ab53212, Abcam, Cambridge, MA), anti-PGC-1 α (sc-518025, Santa Cruz Biotechnology, Texas, USA), anti-mitochondrial cytochrome c oxidase subunit 1 (MT-CO1, ab14705, Abcam) and then analyzed using a streptavidin peroxidase detection system (Maixin Biotech, Fuzhou, China) according to the manufacturer's protocol.

Mitochondrial complex I activity

Mitochondria from kidney cortex were isolated using the mitochondrial isolation kit according to the manufacturer's protocol (ab110168, Abcam). Mitochondrial complex I enzyme activity was measured using the Complex I Enzyme Activity Microplate Assay Kit (ab109721, Abcam). Briefly, isolated mitochondrial samples were loaded to the wells of the microplate at a final protein concentration of 5.5 mg/ml and were incubated for 3 h.

Then, 200 μ l of assay solution was added to each well. Optical density at 450 nm was measured in a kinetic mode for 40 min.

Cell culture and treatment

Human proximal tubular cell line HK2 cell was used for this study. HK2 cells were purchased from American Type Culture Collection and were cultured in Dulbecco's Modified Eagle Medium/F-12 (Hyclone, GE Healthcare Life Science, Logan, UT) supplemented with 10% fetal bovine serum (ScienceCell, San Diego, CA) and 1% penicillin–streptomycin (Gibco, Grand Island, NY). The HK2 cells were cultured in an atmosphere of 5% CO₂ and 21% O₂ and 95% humidity at 37 °C. The HK2 cells were treated with high glucose (HG, 30 mM) under 21% O₂ for 48 h. For TMEM16A specific inhibitor Ani9 (10 μ M) treatment, the HK2 cells were pre-treated for 12 h. For adenoviral (Ad) transfection, HK2 cells grown on chamber slides at 70% confluence were transduced with Ad-NC or Ad-PGC-1 α for 24 h and then exposed to HG for 48 h.

Transmission electron microscopy (TEM)

The renal cortex or HK2 cells were immersed in a fixative that contained 2.5% glutaraldehyde and 4% paraformaldehyde. Sample handling and detection were conducted by the electron microscopic core lab at Southeast University. The mitochondrion in tubules was recorded (H-7650, Hitachi, Japan).

Quantitative real-time polymerase chain reaction (qRT-PCR)

Total RNA was extracted using TRIzol (Takara, Japan). cDNA was synthesized using a PrimeScript RT reagent kit (Takara) according to the manufacturer's instructions. Real-time PCR was performed using an ABI PRISM 7300 real-time PCR System (Applied Biosystems, USA). The relative mRNA expression was normalized to β -actin. All the primers for RT-PCR are listed in Table 1.

Western blot

The protein lysates from the cells or kidney tissues were prepared following standard protocols, and the protein content was examined using a BCA protein assay kit (Thermo Fisher Scientific). Then, the proteins samples were separated by Bis–Tris gel (Invitrogen) and transferred onto polyvinylidene difluoride membranes (Millipore) using a wet-transfer system. The membranes were blocked in 5% BSA in TBS-T (tris buffered saline–Tween 20) for 2 h at room temperature and were incubated with primary antibodies overnight at 4 °C. Next, the membranes were washed and incubated with secondary HRP-conjugated antibodies for 2 h at room temperature, and the signals were detected using an enhanced chemiluminescence advanced system (GE Healthcare). In the study, the primary antibodies used were anti- α -SMA (ab5694, Abcam, Cambridge, MA, USA), anti-Collagen-1 (ab34710, Abcam), anti-FN (ab2413, Abcam), anti-TMEM16A (ab53212, Abcam), anti-PGC-1 α (sc-518025, Santa Cruz Biotechnology, Texas, USA), and anti- β -actin (AY0573, Abways, China). The secondary HRP-conjugated antibodies used were anti-mouse IgG and anti-rabbit IgG (Abcam).

Table 1 Primers used for quantitative RT-PCR

Primer	Forward (5'–3')	Reverse (5'–3')
Ms α -SMA	CAGCAAACAGGAATACGACGAA	AACCACGAGTAACAAATCAAAGC
Ms Collagen-1	GTCAGACCTGTGTGTTCCCTACTCA	TCTCTCCAAACCAGACGTGCTTC
Ms FN	GCAAGAAGGACAACCGAGGAAA	GGACATCAGTGAAGGAGCCAGA
Ms TMEM16A	CTCGTGGTCATCATTCTGCTGG	GCCTTGAAGGTTAGCCTCTCCT
Ms PGC-1 α	CAACCGCAGTCGCAACATG	CCCTTCTTGGTGGAGTGCC
Ms β -actin	GAGACCTTCAACACCCAGC	ATGTCACGCACGATTCCC
Homo α -SMA	ATGGTGATGACCTGCCCGTCT	ACTGAGCGTGGCTACTCCTTCG
Homo Collagen-1	GGTAGGTGATGTTCTGGGAGGC	CAAGAGGCATGTCTGGTTCGG
Homo FN	GGAGCAAATGGCACCGAGATA	GAAGTGGGACCGTCAGGGAGA
Homo TMEM16A	GCAAACATGGAGGACCACTT	GCCGTATTACCAGCCATCAT
Homo PGC-1 α	CCTGTGATGCTTTTGCTGCTCTTG	AAACTATCAAATCCAGAGAGTCA
Homo β -actin	ACTCTTCCAGCCTTCCTTCC	GAGGAGCAATGATCTTGATCTTC

α -SMA α -smooth muscle actin, FN Fibronectin, TMEM16A transmembrane protein 16A, PGC-1 α peroxisome proliferator-activated receptor-gamma coactivator-1 α

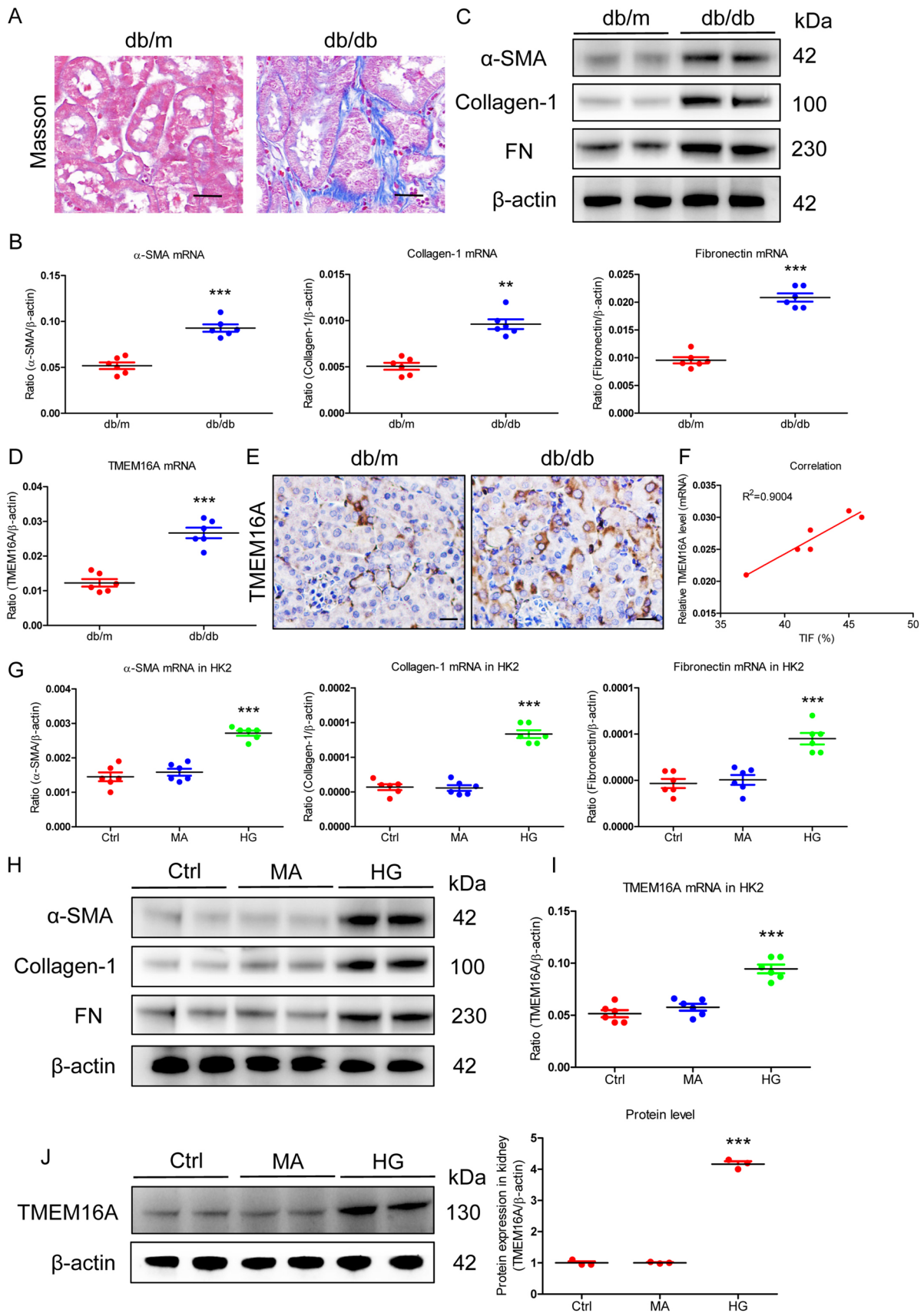


Fig. 1 Increased TMEM16A expression in tubule was associated with TIF in DKD. **A** Histological changes (Masson staining, $n=6$). Scale bar, 50 μm . **B** qRT-PCR analyses of α -SMA ($t=8.146$, $df=5$), Collagen-1 ($t=5.439$, $df=5$), and FN ($t=13.85$, $df=5$) expression ($n=6$). **C** Representative Western blotting of renal α -SMA, Collagen-1, and FN protein expression ($n=6$). **D** qRT-PCR analyses of TMEM16A mRNA expression in renal tissues from db/db mice ($n=6$, $t=7.589$, $df=5$). **E** TMEM16A immunostaining in kidneys from db/db mice. Scale bars, 50 μm . **F** The correlation between TIF percentage and TMEM16A expression level. **G** qRT-PCR analyses of α -SMA ($t=7.713$, $df=5$), Collagen-1 ($t=11.84$, $df=5$), and FN ($t=5.723$, $df=5$) expression in HK2 cells ($n=6$). **H** Representative Western blotting of α -SMA, Collagen-1, and FN protein expression ($n=3$). **I** TMEM16A mRNA expression in HK2 cells ($n=6$, $t=7.138$, $df=5$). **J** Representative Western blotting and quantitative data of TMEM16A protein expression ($n=3$, $t=37.83$, $df=2$). The relative levels were normalized to β -actin for qRT-PCR and Western blotting analyses. Data are mean \pm SEM. ** $P < 0.01$, *** $P < 0.001$ versus db/m (Student's t test) and *** $P < 0.001$ versus Ctrl (one-way analysis of variance followed by Bonferroni's correction)

Statistical analyses

Data are presented as means \pm SEM. For experiments comparing two groups, results were analyzed using a Student's t test or Mann–Whitney U test. When > 2 groups were compared, one-way analysis of variance followed by Bonferroni correction was employed to analyze the differences by SPSS v.20.0 (IBM, Armonk, NY). A two-sided P value of < 0.05 was considered significant.

Results

Tubular TMEM16A expression was associated with TIF in DKD

Histologically, we found that the TIF was significantly increased in the kidney of db/db mice (Fig. 1A). Meanwhile, the mRNA expression of ECM, including α -SMA, Collagen-1 and FN, was also markedly increased (Fig. 1B). ECM protein expression was also detected by Western blotting (Fig. 1C and Supplementary Fig. 1). Then, the TMEM16A expression in DKD was explored. Interestingly, we found that the TMEM16A expression was increased at the transcriptional level (Fig. 1D). Immunohistochemistry analysis revealed that TMEM16A was expressed predominantly in tubule epithelial cells (Fig. 1E). Correlation analysis revealed that TMEM16A expression was positively correlated with TIF percentage in kidney tissues (Fig. 1F). Further, the TMEM16A expression was explored in vitro. As expected, the mRNA and protein expression of ECM in HG-treated HK2 cell were significantly increased (Fig. 1G, H, and Supplementary Fig. 2). Concomitantly, there was a significant increase in mRNA expression of TMEM16A (Fig. 1I), a pattern that was recapitulated by Western blotting

(Fig. 1J). Thus, the TIF was strongly associated with the expression of tubular TMEM16A in the DKD, implying a potential link between TMEM16A expression in tubules and renal TIF responses in the DKD.

TMEM16A inhibition protects against TIF in DKD

To investigate the potential function of TMEM16A on TIF under the condition of DKD, TMEM16A specific inhibitor Ani9 was used to suppress the TMEM16A activation. Interestingly, decreased serum creatinine and urinary albumin levels were found (Supplementary Fig. 3A and 3B). Histologically, we found that the TIF was significantly ameliorated in the kidney of db/db mice with Ani9 administration (Fig. 2A), and markedly ameliorated glomerular injury was observed (Supplementary Fig. 3C). Meanwhile, the mRNA and protein expressions of ECM, including α -SMA, Collagen-1 and FN, were also markedly decreased (Fig. 2B, C, and Supplementary Fig. 4). Further, the potential function of TMEM16A on fibrogenesis was studied in vitro. Interestingly, blockade of TMEM16A activation was significantly decreased ECM expression at transcription levels (Fig. 2D). Consistently, TMEM16A inhibition effectively ameliorated ECM protein expression (Fig. 2E). These data indicated that TMEM16A activation plays a critical role in the development of TIF and blockade of TMEM16A activation ameliorates TIF.

TMEM16A activation induces tubular mitochondrial dysfunction in DKD

Then, the exact mechanism of TMEM16A-induced TIF was studied. Increasing evidence indicated that mitochondrial dysfunction contributes to the development and progression of DKD [10, 11]. Therefore, we hypothesized that TMEM16A activation mediates development of TIF through mitochondrial dysfunction. Firstly, the mitochondrial morphology characterized by mitochondrial swelling, brightened matrix, and disorganized fragmented cristae were observed in the db/db mice (Fig. 3A). Meanwhile, the reduction in MT-CO1 expression (Fig. 3B) and mitochondrial respiratory chain complex I activity (Fig. 3C) were also found. Further, altered mitochondrial morphology characterized by mitochondrial swelling, brightened matrix, and disorganized fragmented cristae were also found in HG-treated HK2 cells (Fig. 3D). Concomitantly, mitochondrial respiratory chain complex I activity was decreased (Fig. 3E), indicating that tubular mitochondrial dysfunction is a characteristic feature of DKD. Interestingly, when the TMEM16A activation was inhibited using the specific inhibitor, the mitochondrial dysfunction was ameliorated markedly, with the evidence of mitochondrial morphology (Fig. 3F), as well as the increased in MT-CO1 expression (Fig. 3G) and

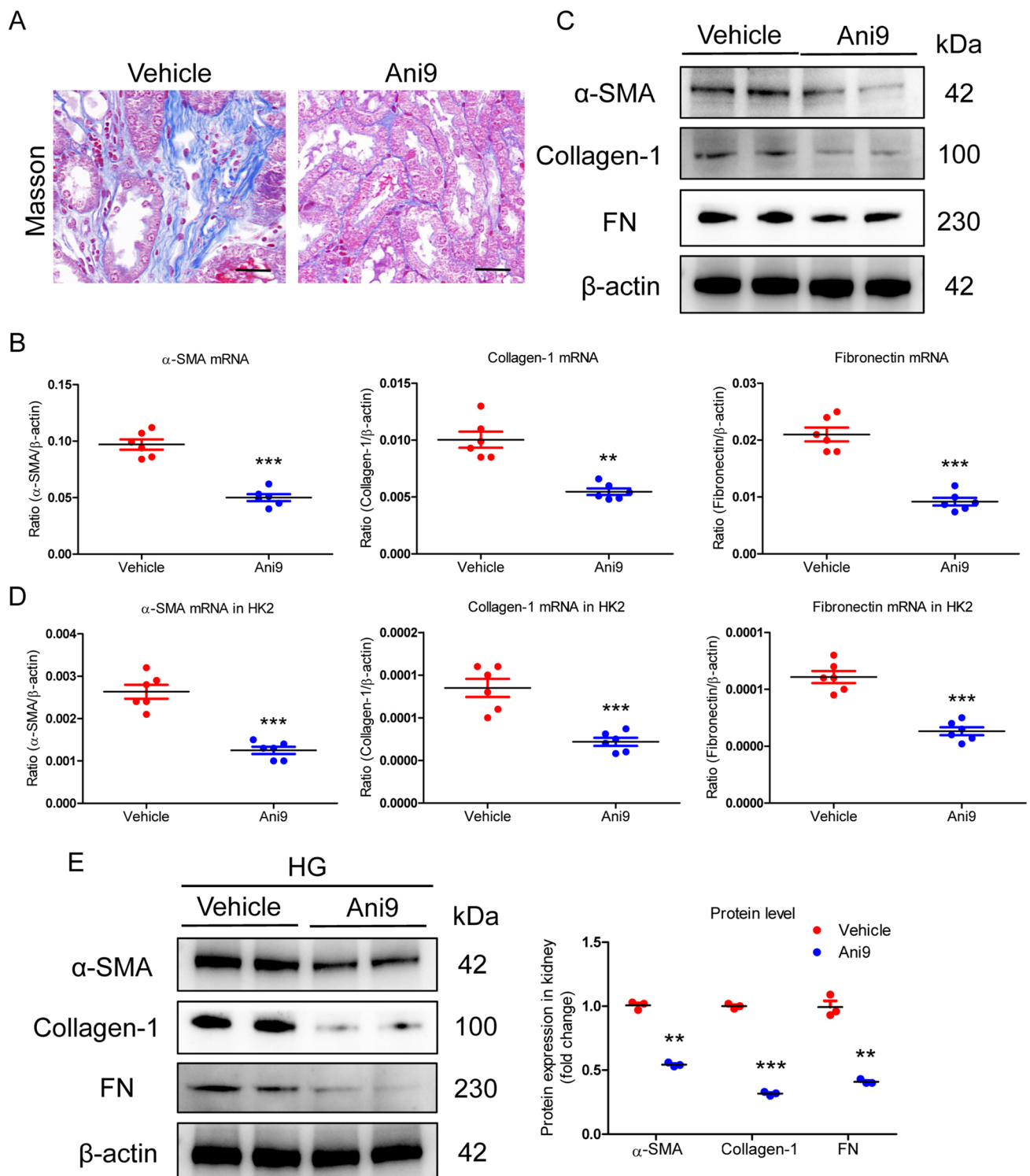


Fig. 2 TMEM16A inhibition protects against TIF in DKD. **A** Histological changes of Masson staining ($n=6$). Scale bar, 50 μm . **B** qRT-PCR analyses of α -SMA ($t=11.58$, $df=5$), Collagen-1 ($t=5.622$, $df=5$), and FN ($t=8.164$, $df=5$) expression in kidneys from db/db mice with TMEM16A inhibitor Ani9 treatment ($n=6$). **C** Representative Western blotting of renal α -SMA, Collagen-1, and FN protein expression ($n=6$). **D** qRT-PCR analyses of α -SMA ($t=9.714$, $df=5$), Collagen-1 ($t=8.112$, $df=5$), and FN ($t=9.088$, $df=5$) expression in

HG-treated HK2 cells with TMEM16A inhibitor Ani9 administration ($n=6$). **E** Representative Western blotting and quantitative data of renal α -SMA ($t=16.98$, $df=2$), Collagen-1 ($t=205.0$, $df=2$), and FN ($t=14.84$, $df=2$) protein expression ($n=3$). The relative levels were normalized to β -actin for qRT-PCR and Western blotting analyses. Data are mean \pm SEM. ** $P < 0.01$, *** $P < 0.001$ versus Vehicle (Student's t test)

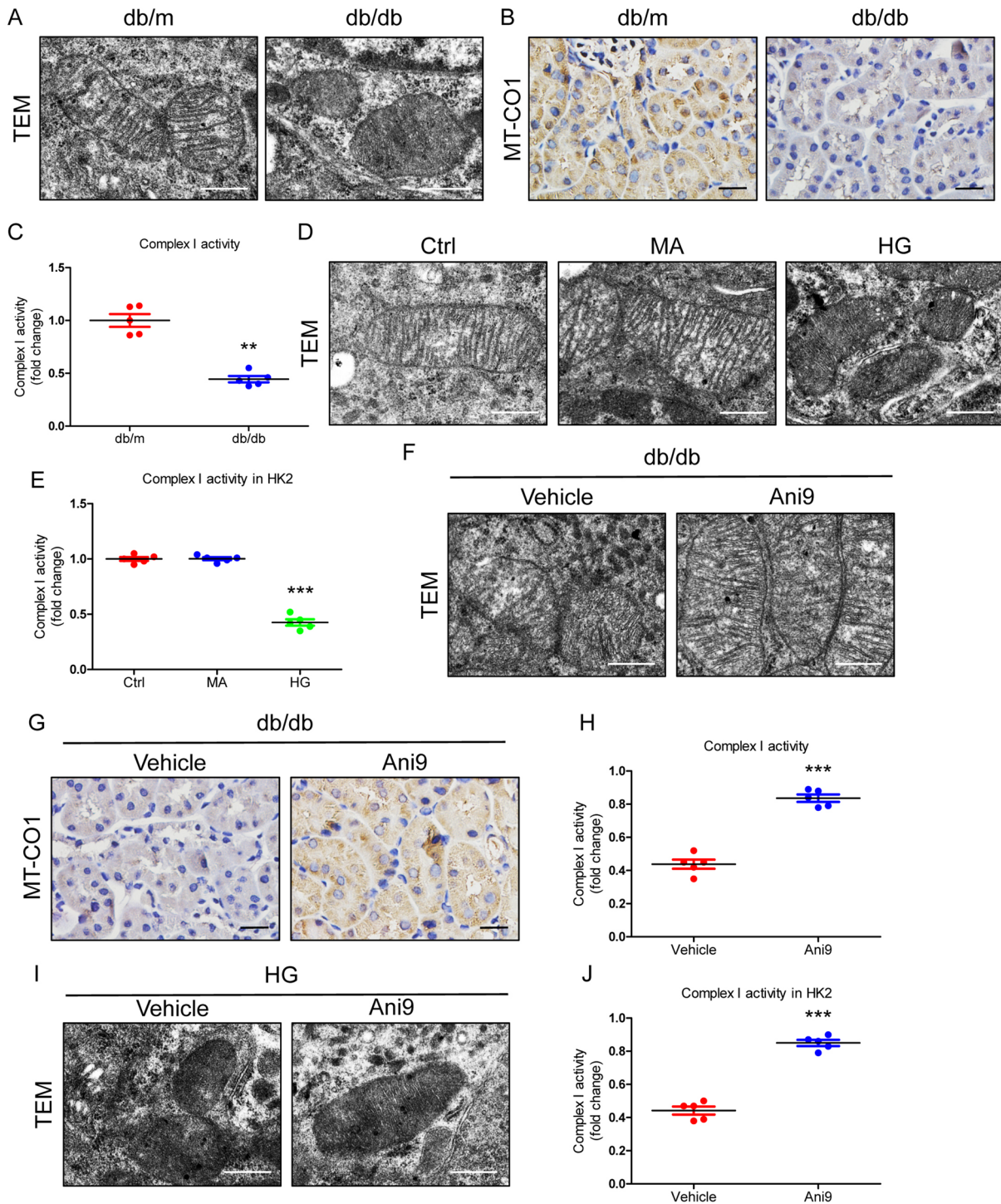


Fig. 3 TMEM16A activation promotes tubular mitochondrial dysfunction in DKD. **A** TEM images of mitochondria in renal tubules. Scale bars, 500 nm. **B** Immunohistochemical analysis of cytochrome c oxidase subunit I (MT-CO1) expression in kidney sections. Scale bars, 50 μ m. **C** Mitochondrial respiratory chain complex I enzymatic activity ($n=5$, $t=7.235$, $df=4$). **D** TEM images of mitochondria in HK2 cells. Scale bars, 500 nm. **E** Mitochondrial respiratory chain complex I enzymatic activity in HK2 cells ($n=5$, $t=19.64$, $df=4$). **F** TEM images of mitochondria in renal tubules from db/db mice with TMEM16A inhibitor Ani9 treatment. Scale bars, 500 nm. **G** Immunohistochemical analysis of MT-CO1 expression in kidney sections

from db/db mice with TMEM16A inhibitor Ani9 treatment. Scale bars, 50 μ m. **H** Mitochondrial respiratory chain complex I enzymatic activity ($n=5$, $t=9.423$, $df=4$). **I** TEM images of mitochondria in HK2 cells with TMEM16A inhibitor Ani9 administration. Scale bars, 500 nm. **J** Mitochondrial respiratory chain complex I enzymatic activity in HK2 cells with TMEM16A inhibitor Ani9 administration ($n=5$, $t=11.21$, $df=4$). Data are mean \pm SEM. *** $P < 0.001$ versus db/m or Vehicle (Student's t test) and ** $P < 0.01$, *** $P < 0.001$ versus Ctrl (one-way analysis of variance followed by Bonferroni's correction)

mitochondrial respiratory chain complex I activity (Fig. 3H). As expected, in the HK2 cells, when the TMEM16A activation was inhibited, the mitochondrial morphology (Fig. 3I) and the mitochondrial respiratory chain complex I activity (Fig. 3J) followed a similar trajectory. Thus, these results demonstrated that the TMEM16A activation plays a crucial role in tubular mitochondrial dysfunction in DKD.

TMEM16A mediated tubular mitochondrial dysfunction by inhibiting PGC-1 α in DKD

Next, the exact molecular mechanism of TMEM16A-induced tubular mitochondrial dysfunction was explored. PGC-1 α is a master regulator of mitochondrial biogenesis and function [12]. We found that the PGC-1 α mRNA expression was significantly decreased in the kidney from DKD mice (Fig. 4A). Immunohistochemistry analysis revealed that PGC-1 α was expressed predominantly in tubule cells (Fig. 4B). Interestingly, when the TMEM16A activation was inhibited, the decreased PGC-1 α expression was ameliorated markedly at both transcription and protein levels (Fig. 4C, D). Further, the functional role of PGC-1 α in TMEM16A-mediated mitochondrial dysfunction was explored in vitro. As expected, the PGC-1 α mRNA expression was decreased (Fig. 4E). PGC-1 α protein level was detected by Western blotting (Fig. 4F). After blockade of TMEM16A, the expression of PGC-1 α in HK2 cells followed a similar trajectory (Fig. 4G, H). These findings indicate that TMEM16A mediated tubular mitochondrial dysfunction by inhibiting PGC-1 α .

Overexpression of PGC-1 α retards TMEM16A-mediated TIF in DKD

To determine the functional effect of PGC-1 α on TMEM16A-mediated TIF, Lv-mediated PGC-1 α overexpression was administered via the tail vein of db/db mice. Histologically, we found that the TIF was significantly ameliorated in the kidney of db/db mice with Lv-PGC-1 α overexpression (Fig. 5A). Meanwhile, the mRNA and protein expressions of ECM, including α -SMA, Collagen-1 and FN, were also markedly decreased (Fig. 5B,C and Supplementary Fig. 5). Concomitantly, the reduction in MT-CO1 expression was ameliorated markedly (Fig. 5D). Further, the potential function of PGC-1 α on TMEM16A-mediated fibrogenesis was studied in vitro. Interesting, PGC-1 α overexpression with adenovirus was significantly decreased ECM expression at both transcription and protein levels in the HG-treated HK2 cells (Fig. 5E,F). Collectively, PGC-1 α dysfunction is the key factor causing TIF and activation of PGC-1 α retards TMEM16A-mediated TIF in DKD.

TMEM16A-induced fibrogenesis is dependent on increased intracellular Cl⁻

To further understand the association between the TMEM16A Cl⁻ channel and TIF, we detected the alteration of intracellular Cl⁻ 48 h after HG treatment in HK2 cells. The result showed that intracellular Cl⁻ was increased from 37.02 ± 0.23 mM at baseline to 39.04 ± 0.24 mM after HG stimulation (Fig. 6A). Interestingly, inhibition of TMEM16A significantly suppressed the HG-induced increase in intracellular Cl⁻ (Fig. 6B), indicating that HG increases intracellular Cl⁻ through TMEM16A. To further understand the impact of Cl⁻ alteration on HG-induced PGC-1 α inhibition and consequent fibrosis, reduced intracellular Cl⁻ was achieved by using low Cl⁻ culture medium. As shown in Fig. 6C, reduction of Cl⁻ effectively maintained PGC-1 α activation. Further, compared with normal Cl⁻ medium, the increase in Collagen-1 and α -SMA expression induced by HG was significantly ameliorated in HK2 cells when were cultured in low Cl⁻ medium (Fig. 6D). Concomitantly, a similar pattern was recapitulated by Western blotting (Fig. 6E). These results demonstrated the critical role of TMEM16A-mediated Cl⁻ in HG-induced fibrogenesis.

Discussion

Emerging evidence indicated that TMEM16A plays a crucial role in the renal pathophysiology. However, the functional effects of TMEM16A on TIF under the condition of DKD remains obscure. In this study, we found that tubular TMEM16A expression was significantly increased, promoting the development of TIF in DKD. Mechanistically, activation of TMEM16A induced mitochondrial dysfunctions through inhibiting PGC-1 α in TIF under the condition of DKD. In addition, TMEM16A-induced fibrogenesis is dependent on increased intracellular Cl⁻. Our findings demonstrate that TMEM16A plays an essential effect on the TIF in DKD. Blockade of TMEM16A activation may serve as a novel therapeutic approach to ameliorate TIF in DKD.

Histology, TIF is the final common pathway of progressive DKD. Increasing evidence found that in response to microenvironment changes, tubules contribute to development of TIF both through autocrine and paracrine effects, indicating that tubule plays a central role in TIF progression [13]. For instance, it is summarized that maladaptive mitochondrial metabolism in tubules, tubular cell senescence, epithelial-mesenchymal transdifferentiation, epigenetic changes in tubules and acquiring pro-inflammatory phenotype are the exact molecular mechanisms that drive DKD [14]. Recently, TMEM16A, a calcium-activated chloride channel, is found to be involved in a variety of vital physiological functions and may be targeted pharmacologically

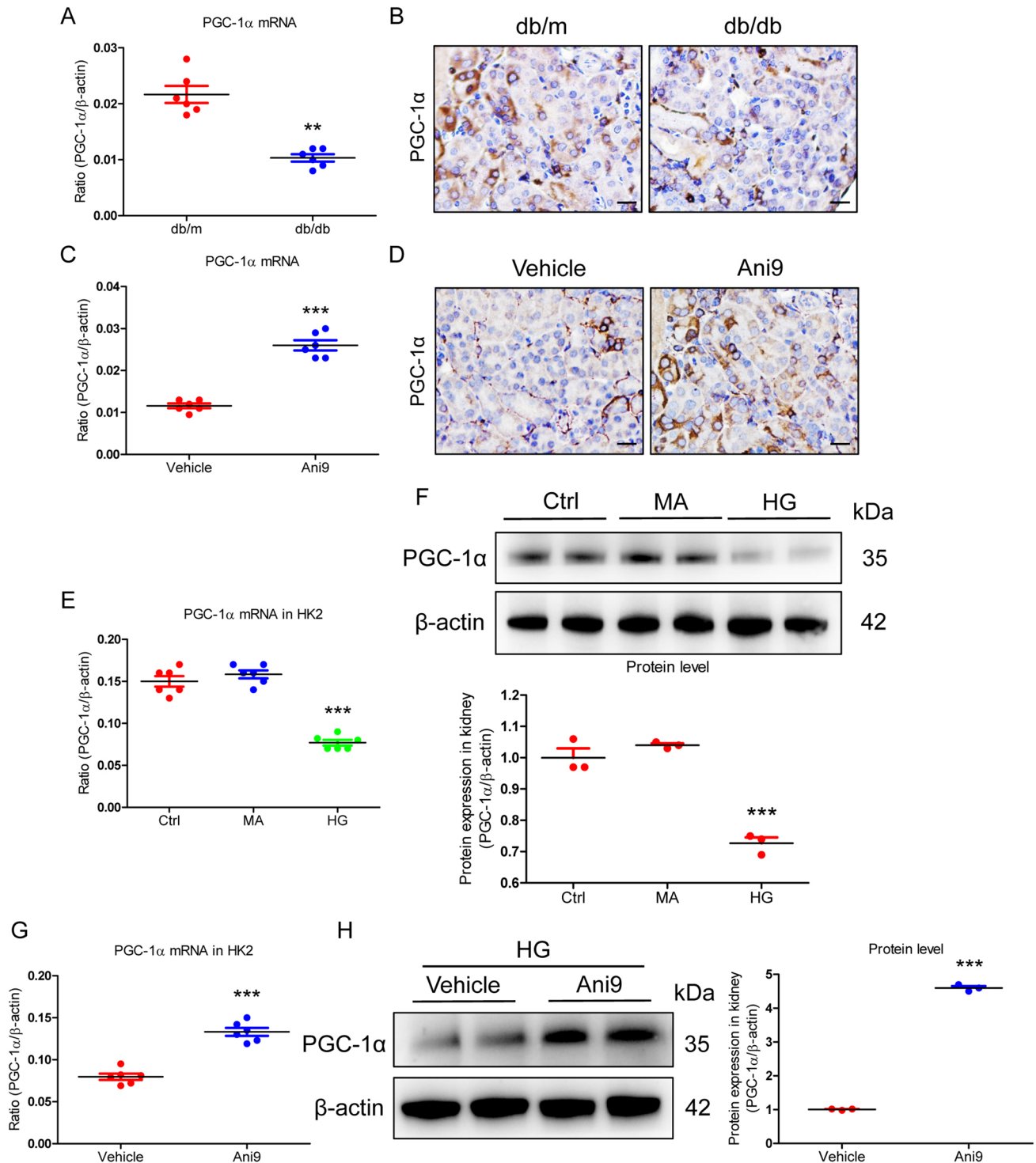


Fig. 4 TMEM16A mediated tubular mitochondrial dysfunction by inhibiting PGC-1 α . **A** qRT-PCR analyses of PGC-1 α expression in the kidney from db/db mice ($n=6$, $t=6.720$, $df=5$). **B** Immunohistochemical analysis of PGC-1 α expression in kidney sections ($n=6$). Scale bars, 50 μ m. **C** PGC-1 α mRNA expression in the kidney from db/db mice with TMEM16A inhibitor Ani9 treatment ($n=6$, $t=10.18$, $df=5$). **D** Immunohistochemical analysis of PGC-1 α expression ($n=6$). Scale bars, 50 μ m. **E** qRT-PCR analysis of PGC-1 α expression in the HG-treated HK2 cell ($n=6$, $t=11.55$, $df=5$). **F** Representative Western blotting and quantitative data

of PGC-1 α protein expression ($n=3$, $t=10.74$, $df=2$). **G** PGC-1 α mRNA expression in the HG-treated HK2 cell with TMEM16A inhibitor Ani9 administration ($n=6$, $t=13.76$, $df=5$). **H** Representative Western blotting and quantitative data of PGC-1 α protein expression ($n=3$, $t=77.0$, $df=2$). The relative levels were normalized to β -actin for qRT-PCR and Western blotting analyses. Data are mean \pm SEM. ** $P < 0.01$, *** $P < 0.001$ versus db/m or Vehicle (Student's t test) and *** $P < 0.001$ versus Ctrl (one-way analysis of variance followed by Bonferroni's correction)

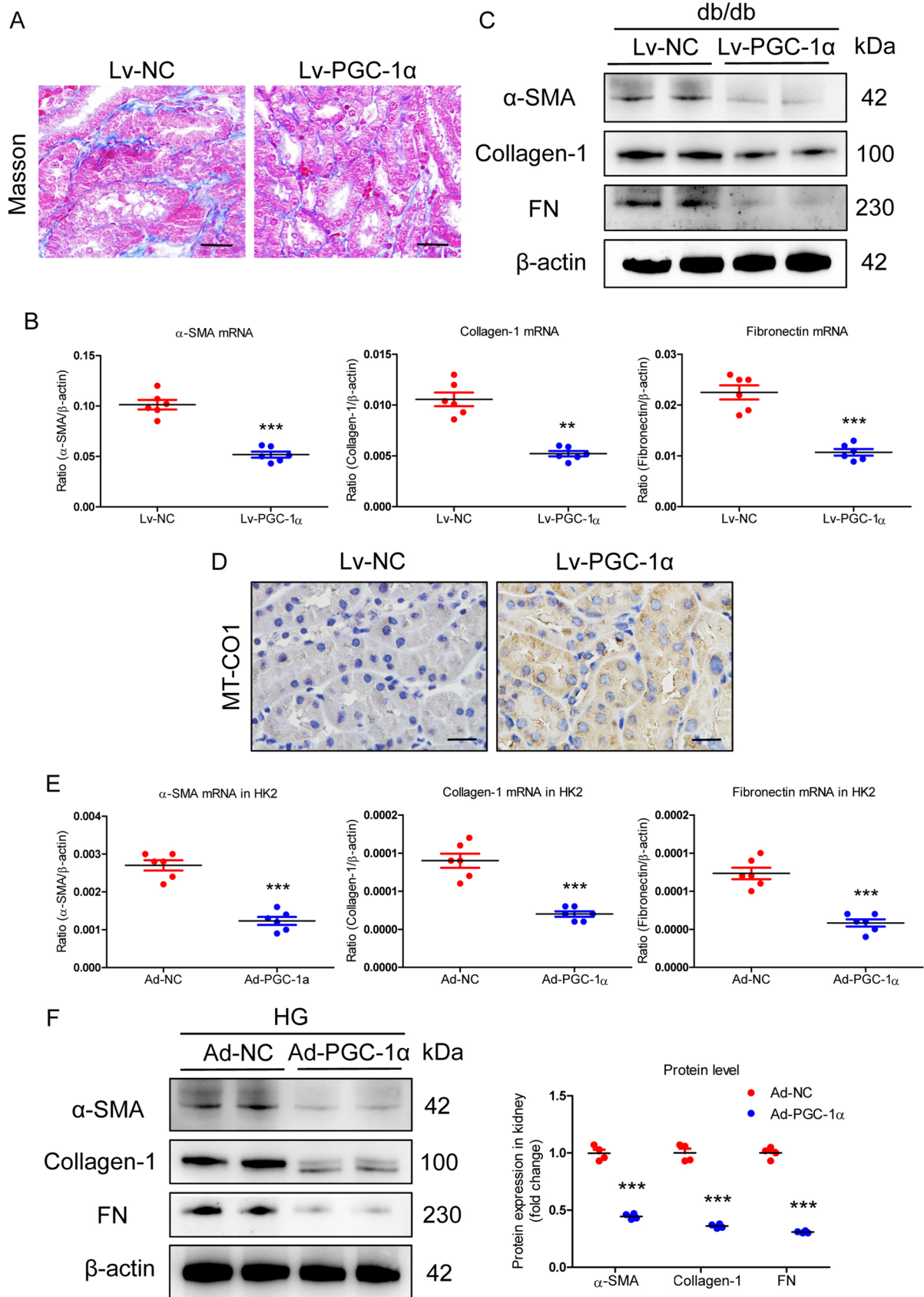


Fig. 5 Overexpression of PGC-1 α retards TMEM16A-mediated TIF in DKD. **A** Histological changes (Masson staining) in db/db mice with Lv administration (n=6). Scale bar, 50 μ m. **B** α -SMA (t=11.63, df=5), Collagen-1 (t=5.996, df=5), and FN (t=7.58, df=5) mRNA expression in the kidney from db/db mice with Lv administration (n=6). **C** Representative Western blotting of renal α -SMA, Collagen-1, and FN protein expression (n=6). **D** Immunohistochemical analysis of MT-CO1 expression (n=6). Scale bar 50 μ m. **E** qRT-PCR analyses of α -SMA (t=9.511, df=5), Collagen-1 (t=8.573, df=5), and FN (t=11.55, df=5) expression in the HG-treated HK2 cell with Ad administration (n=6). **F** Representative Western blotting and quantitative data of α -SMA (t=17.87, df=3), Collagen-1 (t=16.81, df=3), and FN (t=27.38, df=3) protein expression (n=4). The relative levels were normalized to β -actin for qRT-PCR and Western blotting analyses. Data are mean \pm SEM. **P<0.01, ***P<0.001 versus Lv-NC and Ad-NC (Student's t test)

for therapeutic benefit in diseases such as hypertension [15], stroke [16], and cystic fibrosis [17]. Although the determination of the TMEM16A structure and high-throughput screening efforts, and pre-clinical investigations are hastening our understanding of the physiology of this channel, the functional roles in DKD remains poorly understood. Here, we observed upregulated TMEM16A at both the transcription and protein levels in the kidney of DKD, which was induced primarily in tubular cells. More interestingly, our in vivo and in vitro studies indicated that upregulated TMEM16A was involved in the pathophysiology of TIF development under the condition of DKD. It was consistent with previous findings that TMEM16A expression is regulated by multiple signaling pathways including mitogen-activated protein kinase, nuclear factor kappa B (NF- κ B) and transforming growth factor- β in pathological condition [18–20] and tubular TMEM16A contributes to the regulation of renal function [8], implying that tubular TMEM16A plays a pivotal role in the pathogenesis of TIF.

Previously, Li et al. [18] had demonstrated that tubular TMEM16A expression was a critical mechanism to promote fibrogenesis in kidneys of unilateral ureteral obstruction and high-fat diet murine models. Further, TMEM16A is essential for the development of cystic fibrosis and has become a promising therapeutic target for cystic disease [21]. We demonstrated that TIF in DKD is prevented by pharmacological inhibition of TMEM16A in vivo and in vitro. These data showed that TMEM16A promotes TIF. However, the precise regulatory pathway for these effects has not been described in the setting of DKD.

Increasing studies found that mitochondrial dysfunction, a critical pathological feature, is the key instigator of progression of TIF [22], including the DKD. Recently, maintaining mitochondrial energy homeostasis in a variety of kidney diseases by pharmacological and genetic intervention could effectively ameliorate the DKD [23]. Although multiple independent molecular mechanisms have been found to be involved in the regulation

of mitochondrial function, in our studies, we found that tubular mitochondrial dysfunction in DKD was induced by TMEM16A activation. Similarly, Li et al. [24] recently reported that inhibition of TMEM16A improves cisplatin-induced acute kidney injury via preventing mitochondrial fission. To our knowledge, this is the first to discover the relationship between TMEM16A and mitochondrial dysfunction in chronic kidney diseases.

Then, what is the exact mechanism of TMEM16A-mediated tubular mitochondrial dysfunction under the condition of DKD. Previous studies showed that PGC-1 α , a master regulator for mitochondrial function, were found to play an important role in maintaining the physiological function and tissue structure of the kidney [25, 26]. These compelling studies encouraged us to explore a possible role of PGC-1 α in mediating TMEM16A-induced mitochondrial dysfunction. Interestingly, in the present study, we found that mitochondrial dysfunction induced TMEM16A activation depends on the inhibition of PGC-1 α . Because significantly ameliorated TIF was observed in mice by PGC-1 α overexpression administering, which is consistent with previous findings that tubule-specific overexpression of PGC-1 α ameliorates Notch1-induced kidney injury [27]. Additionally, relevant to our findings, Qin et al. [28] identified that promoting PGC-1 α -regulated mitochondrial energy homeostasis protects against DKD. Hence, it is suggested that PGC-1 α -mediated mitochondrial energy homeostasis might be a critical regulator for TMEM16A-induced TIF.

Given that TMEM16A is a calcium-activated chloride channel and Cl $^{-}$ can serve as an intracellular messenger, and alteration of Cl $^{-}$ plays a critical role in a variety of physiological and pathological processes [29, 30], we speculated that TMEM16A contributes to PGC-1 α inhibition and TIF development by regulating Cl $^{-}$. Interestingly, we observed that HG evoked a significant increase of intracellular Cl $^{-}$ in HK2 cells. Meanwhile, we found that HG-induced intracellular Cl $^{-}$ increase was markedly suppressed by inhibition of TMEM16A. Notably, low Cl $^{-}$ dramatically blunted HG-induced PGC-1 α suppression, and collagen-1 and α -SMA expression. To our knowledge, our finding is the first to demonstrate that HG-induced fibrogenesis is Cl $^{-}$ dependent. Further, what is the exact mechanism of Cl $^{-}$ dependent PGC-1 α inhibition? Accumulating evidence indicated that intracellular Cl $^{-}$ concentration plays a critical role in various pathophysiological processes. For instance, Huang W, et al. [29] Found that increased intracellular Cl $^{-}$ concentration improves airway epithelial migration by activating RhoA signaling. Additionally, decrease of intracellular Cl $^{-}$ concentration promotes endothelial cell inflammation by activating NF- κ B pathway [31]. These findings allow us to speculate that the intracellular Cl $^{-}$ concentration involved in the TMEM16A-mediated PGC-1 α inhibition. Taken together, reduction of intracellular Cl $^{-}$ concentration by TMEM16A

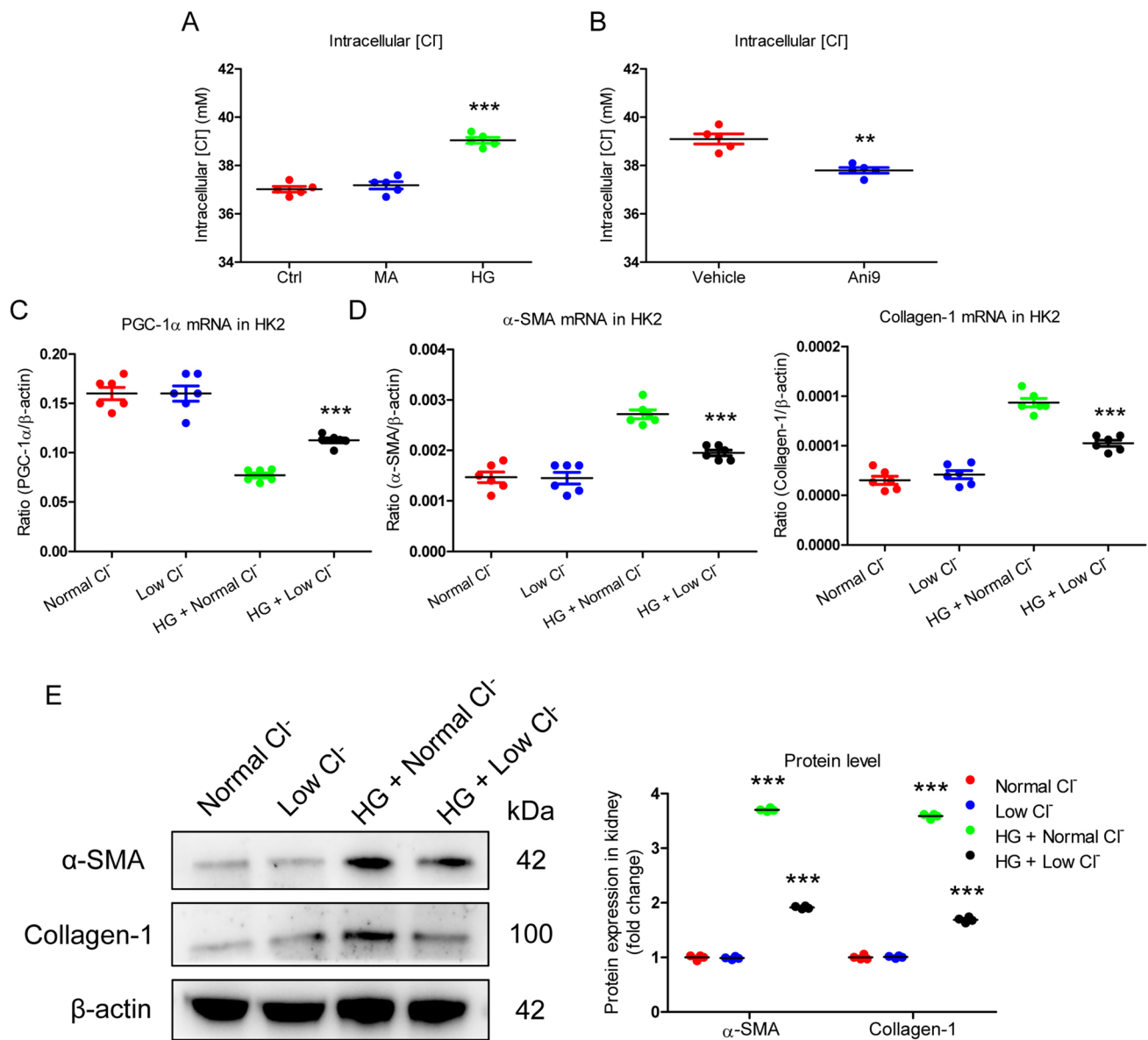


Fig. 6 TMEM16A-induced fibrogenesis is dependent on increased intracellular Cl^- . **A** Intracellular Cl^- concentration in HK2 cells ($n=5$, $t=10.05$, $df=4$). *** $P < 0.001$ versus Ctrl (one-way analysis of variance followed by Bonferroni's correction). **B** Intracellular Cl^- concentration in HG-treated HK2 cells with inhibition of TMEM16A ($n=5$, $t=5.445$, $df=4$). ** $P < 0.01$ versus Vehicle (Student's t test). **C** Decreased Cl^- concentration by low Cl^- medium reduced HG-mediated PGC-1 α expression ($n=6$, $t=4.747$, $df=5$). *** $P < 0.001$ versus HG + normal Cl^- treatment group (one-way analysis of vari-

ance followed by Bonferroni's correction). **D** Low Cl^- medium inhibited HG-mediated increase of α -SMA ($t=5.791$, $df=5$) and Collagen-1 ($t=7.424$, $df=5$) expression ($n=6$). *** $P < 0.001$ versus HG + normal Cl^- treatment group (one-way analysis of variance followed by Bonferroni's correction). **E** Representative Western blotting and quantitative data of α -SMA ($t=80.91$, $df=2$), and Collagen-1 ($t=69.04$, $df=2$) protein expression ($n=3$). *** $P < 0.001$ versus normal Cl^- or HG + normal Cl^- (one-way analysis of variance followed by Bonferroni's correction)

inhibition may be the exact mechanism for preventing progression of DKD.

Finally, we realized that there is some limitation for this study. Our findings mainly based on the male mice. Given that sex and gender differences are important considerations in the pathogenesis, prognostication and management of DKD [32], the effect and mechanism of the

TMEM16A-PGC-1 α pathway on female still needs to be investigated.

In summary, we have discovered an important role for tubular TMEM16A in inciting TIF in the DKD via suppressing PGC-1 α -mediated mitochondrial homeostasis. Meanwhile, TMEM16A-mediated mitochondrial dysfunction and development of TIF is intracellular Cl^- dependent.

These findings provide unique insights into interdigitating mechanisms of TIF development under the condition of DKD. Blockade of TMEM16A signaling cascade may represent a promising therapeutic approach to ameliorate TIF.

Supplementary Information The online version contains supplementary material available at <https://doi.org/10.1007/s00018-023-05000-6>.

Acknowledgements This study was supported by the grants from the National Natural Science Foundation of China (82000648); the Natural Science Foundation of Jiangsu Province (BK20200363); the Outstanding Youth Cultivation Foundation of Southeast University (2021ZDYYPY07); the Fundamental Research Funds for the Central Universities (2242023K40046); the Innovative and Entrepreneurial Talent (Doctor) of Jiangsu Province; the Natural Science Foundation of Shandong Province (ZR2022MH161); the Science and Technology Planning Projects of Qingdao (2021-WJZD189 and 16-6-2-20-snh); and the Clinical Medicine + X Project of Affiliated Hospital of Qingdao University (3390).

Author contributions JLL, and JYL designed the study, carried out the experiments, and analyzed the data; JXL, CCL, YZ, and AQZ analyzed the data, made the figures, and edited the paper; ZLL, RXM, and HL analyzed the data, made the figures, and wrote and edited the paper. All authors approved the final version of the paper.

Funding The authors have not disclosed any funding.

Availability of data and materials The data that support the findings of this study are available on request from the corresponding author.

Declarations

Conflict of interest The authors declare no competing financial interests.

Ethical approval All animal experimental procedures were approved by the Ethics Review Committee for Animal Experimentation of Southeast University and were performed in accordance with the guidelines established by the National Institutes of Health for the Care and Use of Laboratory Animals.

Consent to participate Not applicable.

References

- Barrera-Chimal J, Lima-Posada I, Bakris GL, Jaisser F (2022) Mineralocorticoid receptor antagonists in diabetic kidney disease-mechanistic and therapeutic effects. *Nat Rev Nephrol* 18(1):56–70
- Rayego-Mateos S, Rodrigues-Diez RR, Fernandez-Fernandez B, Mora-Fernández C, Marchant V, Donate-Correa J, Navarro-González JF, Ortiz A, Ruiz-Ortega M (2023) Targeting inflammation to treat diabetic kidney disease: the road to 2030. *Kidney Int* 103(2):282–296
- Alicic RZ, Rooney MT, Tuttle KR (2017) Diabetic kidney disease: challenges, progress, and possibilities. *Clin J Am Soc Nephrol* 12(12):2032–2045
- Cui X, Shi E, Li J, Li Y, Qiao Z, Wang Z, Liu M, Tang W, Sun Y, Zhang Y, Xie Y, Zhen J, Wang X, Yi F (2022) GPR87 promotes renal tubulointerstitial fibrosis by accelerating glycolysis and mitochondrial injury. *Free Radic Biol Med* 189:58–70
- Chen J, Wang X, He Q, Bulus N, Fogo AB, Zhang MZ, Harris RC (2020) YAP activation in renal proximal tubule cells drives diabetic renal interstitial fibrogenesis. *Diabetes* 69(11):2446–2457
- Liu Y, Liu Z, Wang K (2021) The Ca²⁺-activated chloride channel ANO1/TMEM16A: an emerging therapeutic target for epithelium-originated diseases? *Acta Pharm Sin B* 11(6):1412–1433
- Huang F, Rock JR, Harfe BD, Cheng T, Huang X, Jan YN, Jan LY (2009) Studies on expression and function of the TMEM16A calcium-activated chloride channel. *Proc Natl Acad Sci USA* 106(50):21413–21418
- Faria D, Rock JR, Romao AM, Schweda F, Bandulik S, Witzgall R, Schlatter E, Heitzmann D, Pavenstädt H, Herrmann E, Kunzelmann K, Schreiber R (2014) The calcium-activated chloride channel Anoctamin 1 contributes to the regulation of renal function. *Kidney Int* 85(6):1369–1381
- Cabrita I, Kraus A, Scholz JK, Skoczynski K, Schreiber R, Kunzelmann K, Buchholz B (2020) Cyst growth in ADPKD is prevented by pharmacological and genetic inhibition of TMEM16A in vivo. *Nat Commun* 11(1):4320
- Yao L, Liang X, Qiao Y, Chen B, Wang P, Liu Z (2022) Mitochondrial dysfunction in diabetic tubulopathy. *Metabolism* 131:155195
- Xie Y, Jing E, Cai H, Zhong F, Xiao W, Gordon RE, Wang L, Zheng YL, Zhang A, Lee K, He JC (2022) Reticulon-1A mediates diabetic kidney disease progression through endoplasmic reticulum-mitochondrial contacts in tubular epithelial cells. *Kidney Int* 102(2):293–306
- Fontecha-Barriuso M, Martin-Sanchez D, Martinez-Moreno JM, Monsalve M, Ramos AM, Sanchez-Niño MD, Ruiz-Ortega M, Ortiz A, Sanz AB (2020) The role of PGC-1 α and mitochondrial biogenesis in kidney diseases. *Biomolecules* 10(2):347
- Gewin LS (2018) Renal fibrosis: primacy of the proximal tubule. *Matrix Biol* 68–69:248–262
- Crottès D, Jan LY (2019) The multifaceted role of TMEM16A in cancer. *Cell Calcium* 82:102050
- Cil O, Chen X, Askew Page HR, Baldwin SN, Jordan MC, Myat Thwe P, Anderson MO, Haggie PM, Greenwood IA, Roos KP, Verkman AS (2021) A small molecule inhibitor of the chloride channel TMEM16A blocks vascular smooth muscle contraction and lowers blood pressure in spontaneously hypertensive rats. *Kidney Int* 100(2):311–320
- Korte N, Ilkan Z, Pearson CL, Pfeiffer T, Singhal P, Rock JR, Sethi H, Gill D, Attwell D, Tammaro P (2022) The Ca²⁺-gated channel TMEM16A amplifies capillary pericyte contraction and reduces cerebral blood flow after ischemia. *J Clin Invest* 132(9):e154118
- Cabrita I, Buchholz B, Schreiber R, Kunzelmann K (2020) TMEM16A drives renal cyst growth by augmenting Ca²⁺ signaling in M1 cells. *J Mol Med (Berl)* 98(5):659–671
- Li XL, Liu J, Chen XS, Cheng LM, Liu WL, Chen XF, Li YJ, Guan YY, Zeng X, Du YH (2022) Blockade of TMEM16A protects against renal fibrosis by reducing intracellular Cl⁻ concentration. *Br J Pharmacol* 179(12):3043–3060
- Mohandes S, Doke T, Hu H, Mukhi D, Dhillon P, Susztak K (2023) Molecular pathways that drive diabetic kidney disease. *J Clin Invest* 133(4):e165654
- Tuttle KR, Agarwal R, Alpers CE, Bakris GL, Brosius FC, Kolkhof P, Uribarri J (2022) Molecular mechanisms and therapeutic targets for diabetic kidney disease. *Kidney Int* 102(2):248–260
- Galiotta LJ (2022) TMEM16A (ANO1) as a therapeutic target in cystic fibrosis. *Curr Opin Pharmacol* 64:102206
- Li X, Xu L, Hou X, Geng J, Tian J, Liu X, Bai X (2019) Advanced oxidation protein products aggravate tubulointerstitial fibrosis through protein kinase C-dependent mitochondrial injury in early diabetic nephropathy. *Antioxid Redox Signal* 30(9):1162–1185
- Forbes JM, Thorburn DR (2018) Mitochondrial dysfunction in diabetic kidney disease. *Nat Rev Nephrol* 14(5):291–312

24. Li XL, Liu XW, Liu WL, Lin YQ, Liu J, Peng YS, Cheng LM, Du YH (2023) Inhibition of TMEM16A improves cisplatin-induced acute kidney injury via preventing DRP1-mediated mitochondrial fission. *Acta Pharmacol Sin* (**Online ahead of print**)
25. Lin J, Wu PH, Tarr PT, Lindenberg KS, St-Pierre J, Zhang CY, Mootha VK, Jäger S, Vianna CR, Reznick RM, Cui L, Manieri M, Donovan MX, Wu Z, Cooper MP, Fan MC, Rohas LM, Zavacki AM, Cinti S, Shulman GI, Lowell BB, Krainc D, Spiegelman BM (2004) Defects in adaptive energy metabolism with CNS-linked hyperactivity in PGC-1 α null mice. *Cell* 119(1):121–135
26. Nam BY, Jhee JH, Park J, Kim S, Kim G, Park JT, Yoo TH, Kang SW, Yu JW, Han SH (2022) PGC-1 α inhibits the NLRP3 inflammasome via preserving mitochondrial viability to protect kidney fibrosis. *Cell Death Dis* 13(1):31
27. Han SH, Wu MY, Nam BY, Park JT, Yoo TH, Kang SW, Park J, Chinga F, Li SY, Susztak K (2017) PGC-1 α protects from notch-induced kidney fibrosis development. *J Am Soc Nephrol* 28(11):3312–3322
28. Qin X, Jiang M, Zhao Y, Gong J, Su H, Yuan F, Fang K, Yuan X, Yu X, Dong H, Lu F (2020) Berberine protects against diabetic kidney disease via promoting PGC-1 α -regulated mitochondrial energy homeostasis. *Br J Pharmacol* 177(16):3646–3661
29. Huang W, Tan M, Wang Y, Liu L, Pan Y, Li J, Ouyang M, Long C, Qu X, Liu H, Liu C, Wang J, Deng L, Xiang Y, Qin X (2020) Increased intracellular Cl⁻ concentration improves airway epithelial migration by activating the RhoA/ROCK Pathway. *Theranostics* 10(19):8528–8540
30. Bazúa-Valenti S, Chávez-Canales M, Rojas-Vega L, González-Rodríguez X, Vázquez N, Rodríguez-Gama A, Argaiz ER, Melo Z, Plata C, Ellison DH, García-Valdés J, Hadchouel J, Gamba G (2015) The effect of WNK4 on the Na⁺-Cl⁻ cotransporter is modulated by intracellular chloride. *J Am Soc Nephrol* 26(8):1781–1786
31. Yang H, Huang LY, Zeng DY, Huang EW, Liang SJ, Tang YB, Su YX, Tao J, Shang F, Wu QQ, Xiong LX, Lv XF, Liu J, Guan YY, Zhou JG (2012) Decrease of intracellular chloride concentration promotes endothelial cell inflammation by activating nuclear factor- κ B pathway. *Hypertension* 60(5):1287–1293
32. Sridhar VS, Yau K, Benham JL, Campbell DJT, Cherney DZI (2022) Sex and gender related differences in diabetic kidney disease. *Semin Nephrol* 42(2):170–184

Publisher's Note Springer Nature remains neutral with regard to jurisdictional claims in published maps and institutional affiliations.

Springer Nature or its licensor (e.g. a society or other partner) holds exclusive rights to this article under a publishing agreement with the author(s) or other rightsholder(s); author self-archiving of the accepted manuscript version of this article is solely governed by the terms of such publishing agreement and applicable law.